

A Study on the Power Control of Wind Energy Conversion System

Mehdi Nafar, Mohammad Reza Mansouri

Abstract—The present research presents a direct active and reactive power control (DPC) of a wind energy conversion system (WECS) for the maximum power point tracking (MPPT) based on a doubly fed induction generator (DFIG) connected to electric power grid. The control strategy of the Rotor Side Converter (RSC) is targeted in extracting a maximum of power under fluctuating wind speed. A fuzzy logic speed controller (FLC) has been used to ensure the MPPT. The Grid Side Converter is directed in a way to ensure sinusoidal current in the grid side and a smooth DC voltage. To reduce fluctuations, rotor torque and voltage use of multilevel inverters is a good way to remove the rotor harmony.

Keywords—DFIG, power quality improvement, wind energy conversion system, WECS, fuzzy logic, RSC, GSC, inverter.

I. INTRODUCTION

WIND energy refers to one of the most propitious renewable energy sources due to the progress witnessed in the last decades. WECS with its distinctive structure, management and easy maintenance has attracted governments. With an average global annual growth rate of 14% for the period 2002-2006, wind energy is playing a major role in the effort to increase the share of renewable energy sources in the world energy mix [1], [2], helped for satisfying global energy demand, offering the best opportunity to unlock a new age of environmental protection [3], whereby the world energy crises can be solved in future.

A large attention has paid to DFIG, i.e. one of preferred technology for wind power generation. The use of DFIG in a wind turbine, in comparison with a full rated converter system, represents abundant advantages including reduction of inverter cost, the potential to control torque and a slight increase in efficiency of wind energy extraction. For a variety of reasons, the wind turbines variable-speed operation has been used, including acoustic noise reduction, decrease of the stresses on the mechanical structure and the possibility of active and reactive power control [4]. Most of the major wind turbine manufacturers are developing new larger wind turbines in the 3-6 MW range. With pitch control, huge wind turbines are grounded on variable speed operation through a DFIG or a direct-driven synchronous generator. The power electronics equipment only bears the fraction of the total power for 20-30% [5], i.e. the losses in the power electronics converters and also the costs are reduced. It reduces the stress

in the mechanical structure, reduces the acoustic noise makes it possible to regulate the power [5]. Another advantage of the DFIG system is that the back to back PWM converters, connected between the grid and the induction machine rotor circuit, are sized only for a part of the full power of the generator (about 30). The wind turbine generators can gain the maximum wind power provided at various wind speeds by regulating the shaft speed in a proper way [7].

There exist three common MPPT techniques including The Wind Speed Measurement (WSM) method, Perturbation and Observation (P&O) method and Power Signal Feedback (PSF) method [8]. It should measure shaft speed and wind velocity in the WSM method. Further, the tip-speed-ratio must be determined. There exist two disadvantages on performing the WSM method [9]. First, gaining exact value of the wind velocity is complicated and using the mechanical sensor to measure the shaft speed increases the systems cost. Secondly, the optimal tip speed ratio depends on the wind energy system characteristics [10]. Preceding information on the wind turbine power to maximum level is not required in P&O method at both electric machine parameters and various wind velocities [10], [11]. The P&O method is not proper for medium and large inertia wind turbine systems, but proper for wind turbines with small inertia, as the P&O method causes a delay to the system control [12]. The P&O based strategy is simple, although it could be slow in response to fast changes in wind speed. As a consequence, the WECS may not be capable to operate at the maximum power point throughout the possible wind speed variations. Hence the advantages of the WECS will not be utilized, in spite of the increased capital investment because of the power electronics converter [13].

The controller uses information on the wind turbine maximum power curve so as to execute PSF control. Then the maximum power is routed by shaft speeds control. Wind velocity measurement is not required with this method [12]. Usually, measurement of the power vs. turbine speed curves is required. In the industry, Proportional (P), Proportional Integral (PI) and Proportional Integral Derivative (PID) controllers are widely used due to their simple structures and ease of use in wide range of applications. However, these controllers are tuned for specific linearized models.

The DFIG control schemes are based on concept of vector control with Sliding Mode Control as proposed in [14]. SMC of Active and Reactive Power of a DFIG and extraction of maximum power for Variable Speed by WECS are displayed in [15], [16]. Many researches are conducted on decoupled control of DFIG in order to improve power quality for WECS. In [17], [18] have studied an enhanced control of DFIG and

Nafar. Mehdi, is with the Department of Electrical Engineering, Marvdasht Branch, Islamic Azad University, Marvdasht, Iran

Mansouri. Mohammad Reza, is with the Department of Electrical Engineering, Lamerd Branch, Islamic Azad University, Lamerd, Iran (e-mail: tohid2439@gmail.com).

power quality improvement. In [19], [20], a comparison of FACTS devices (i.e. STATCOM and SVC) for the voltage stability issues is presented. In this paper, to ensure the MPPT, a FLC has been used. The Grid Side Converter is directed in a way to ensure sinusoidal current in the grid side and a smooth DC voltage. To reduce fluctuations, rotor torque and voltage use of multilevel inverters is a good way to remove the rotor harmony.

II. WIND ENERGY CONVERSION SYSTEM

Fig. 1 presents a WECS in which DFIG has been used. From the viewpoint of system, the conversion chain can be classified into two main subsystems which will be separately modeled: a. Aerodynamic Subsystem (wind turbine and gearbox), b. Electrical Subsystem (DFIG).

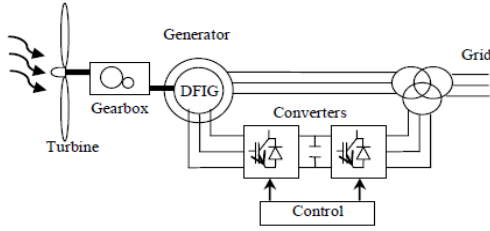


Fig. 1 Wind energy conversion chain

Wind turbine generation system converts power from the kinetic energy of the wind, so it can be expressed as the kinetic power available in the stream of air multiplied by a C_p factor called power coefficient or Betz' s factor. The aerodynamic power is given by:

$$P_{aer} = \frac{1}{2} C_p(\lambda, \beta) \rho S V^3 \quad (1)$$

where ρ , R and V represent the air density, the blade length and the wind velocity, respectively. A wind turbine can only convert just a certain percentage of the captured wind power. This percentage is represented by $C_p(\lambda)$ which is function of the wind speed, the turbine speed and the pitch angle of specific wind turbine blades [5], [6], C_p is dependent on the ratio between the turbine shaft speed Ω and the wind speed V , however this equation seems simple. This ratio is called the tip speed ratio:

$$\lambda = \frac{\Omega_t}{V} \quad (2)$$

The typical C_p versus curve for difference values of pitch Angle β is shown in Fig. 2. In a wind turbine, there is an optimum value of tip speed ratio for which C_p is maximum and that maximizes the power for a given wind speed. The peak power is maximized for each wind speed that has occurred at the point where C_p . To increase the generated power, it is desirable for the generator to have a power characteristic that will follow the maximum C_{pmax} . Fig. 2, showing the relation between C_p , β and λ .

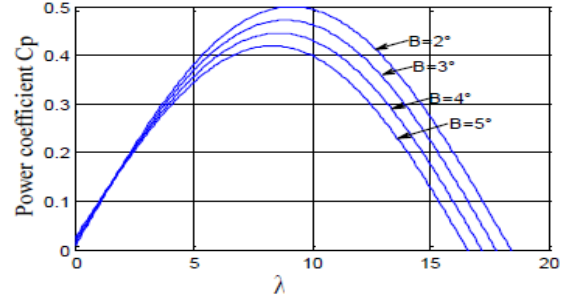


Fig. 2 Power coefficient variation against tip speed ratio and pitch angle

The turbine torque is the ratio of the aerodynamic power to the turbine shaft speed Ω :

$$T_{aer} = \frac{P_{aer}}{\Omega_t} \quad (3)$$

Gear ratio G is set to the generator shaft speed within a desired speed range and the turbine is connected to the generator shaft. Regardless of the transmission losses, the torque and shaft speed of the wind turbine, referred to the generator side of the gearbox, are given by:

$$T_g = \frac{T_{aer}}{G}, \Omega_g = \frac{\Omega_g}{G} \quad (4)$$

where T_g is the torsion of the generator and Ω_g is the generator shaft speed. For low wind speeds, the MPPT is desired so that the output power can be maximized according to the specific wind speed. For high wind speeds, the pitch angle regulation should be achieved to keep the output power at its rated value. For the MPPT objective, it is possible to control the DFIG torque so that the speed of the turbine rotor can be varied proportional to the wind speed. In this way, the optimal tip speed ratio can be maintained, and thus the maximum power coefficient as well as the maximum output power can be achieved. The pitch angle control in a WTGS is used to regulate the pitch angle when the captured wind power exceeds its rated value, or the wind speed exceeds its rated value. Therefore, the output power can be kept at rated value even when the wind speed experiences gusts.

III. MODELLING OF THE DFIG WITH STATOR FIELD ORIENTATION

A typical configuration of a DFIG wind turbine is shown in Fig. 1. A wound-rotor induction generator with slip-rings is used to transmit current between the converter and the rotor windings and variable-speed operation is obtained by injecting a controllable voltage in to the rotor at the desired slip frequency. It is used to generate electrical power at constant frequency whatever wind and shaft speed conditions. The rotor winding is fed through a variable-frequency power converter, typically based on two AC/DC IGBT-based Voltage Source Converters (VSCs), and linked through a DC bus. The variable-frequency rotor supply from the converter enables the rotor mechanical speed to be decoupled from the

synchronous frequency of the electrical network, thereby allowing variable-speed operation of the wind turbine [10]. The equations for a DFIG are identical with a squirrel-cage induction generator except for the rotor voltages are not zeros. The expressions associated to the voltages with the currents

and fluxes across the stator winding in the PARK frame are written as follows through faraday's law and ohm's law [11]: Fig. 3 shows the equivalent circuit of induction machine with dq axis in the arbitrary reference frame. By using the dq model, three to two phase representations are described.

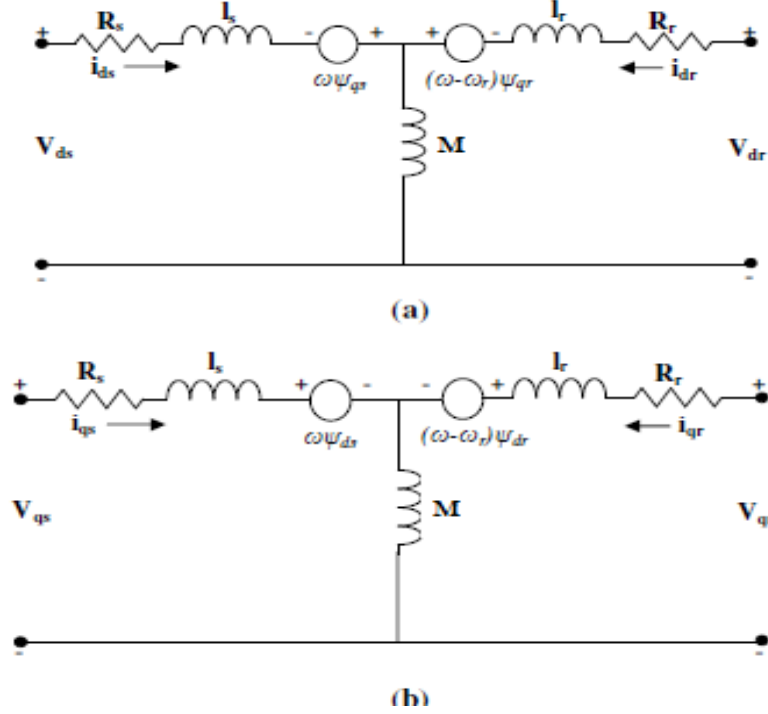


Fig. 3 Equivalent circuit of induction machine in the arbitrary reference frame (a) d axis equivalent circuit (b) q axis equivalent circuit..

The DFIG voltage and flux equations, expressed in the Park reference frame, are given by [11]:

$$\begin{cases} v_{qs} = \frac{d\psi_{qs}}{dt} + R_s i_{qs} + w_s \psi_{ds} \\ v_{ds} = \frac{d\psi_{ds}}{dt} + R_s i_{ds} - w_s \psi_{qs} \\ v_{qr} = \frac{d\psi_{qr}}{dt} + (w_s - w_r) \psi_{dr} + R_r i_{qr} \\ v_{dr} = \frac{d\psi_{dr}}{dt} - (w_s - w_r) \psi_{qr} + R_r i_{dr} \end{cases} \quad (5)$$

where R_s and R_r are, respectively, the stator and rotor phase resistances. L_s , L_r , M , Stator and rotor per phase winding and magnetizing inductances $w = P\Omega_{mec}$. w is the electrical speed and P is the pair pole number.

$$\begin{cases} \psi_{ds} = L_s i_{ds} + M i_{dr} \\ \psi_{qs} = L_s i_{qs} + M i_{qr} \\ \psi_{dr} = L_r i_{dr} + M i_{ds} \\ \psi_{qr} = L_r i_{qr} + M i_{qs} \end{cases} \quad (6)$$

where i_{ds} , i_{qs} , i_{dr} and i_{qr} are, respectively, the direct and quadrature stator and rotor current. The active and reactive powers at the stator, as well as those provide for grid are defined as:

$$\begin{cases} P_s = \frac{3}{2} (v_{ds} i_{ds} + v_{qs} i_{qs}) \\ Q_s = \frac{3}{2} (v_{qs} i_{ds} - v_{ds} i_{qs}) \end{cases} \quad (7)$$

The electromagnetic torque is expressed as:

$$T_{em} = 1.5 (i_{qs} \psi_{ds} - i_{ds} \psi_{qs}) \quad (8)$$

The stator resistance of the DFIG is neglected and the stator flux is set aligned with the d axis and assumed to be constant (it is the case of a powerful and stable grid) [12].

Then, one can write $\psi_{ds} = \psi_s$ and $\psi_{qs} = 0$. Consequently, (5)-(7) become respectively in the steady state regime:

$$\begin{cases} v_{ds}=0 \\ v_{qs} = v_s \approx w_s \psi_s \\ \psi_s = L_s i_{ds} + M i_{dr} \\ 0 = L_s i_{qs} + M i_{qr} \end{cases} \quad (9)$$

$$T_{em} = -\frac{3}{2} P \frac{M}{L_s} \psi_s i_{qr} \quad (10)$$

Perhaps stator resistance is neglected, which is a realistic approximation for medium power machines used in WECS; the stator voltage vector is consequently in quadrature advance in comparison with the stator flux vector.

By using (5) and (9), the rotor voltages are:

$$\begin{cases} v_{dr} = \sigma L_r \frac{di_{dr}}{dt} + R_r i_{dr} - \sigma L_r \omega_r i_{qr} + \frac{M}{L_s} \frac{d\psi_{ds}}{dt} \\ v_{qr} = \sigma L_r \frac{di_{qr}}{dt} + R_r i_{qr} + \sigma L_r \omega_r i_{dr} + s \frac{M}{L_s} V_s \\ \sigma = 1 - \frac{M^2}{L_s L_r} \end{cases} \quad (11)$$

where V_s is the stator voltage magnitude assumed to be constant and s is the slip range, the rotor voltages are obtained:

$$\begin{cases} v_{dr} = \sigma L_r \frac{di_{dr}}{dt} + R_r i_{dr} + f_{em_d} \\ v_{qr} = \sigma L_r \frac{di_{qr}}{dt} + R_r i_{qr} + f_{em_q} \\ f_{em_q} = \sigma L_r \omega_r i_{dr} + s \frac{M}{L_s} V_s \\ f_{em_d} = -\sigma L_r \omega_r i_{qr} \end{cases} \quad (12)$$

where f_{em_d} and f_{em_q} are the crosses coupling terms between

the d axis and q axis.

Using (4), (7) and (9) the stator active and reactive power can then be expressed only versus these rotors

$$\begin{cases} P_s = -\frac{3V_s M}{2L_s} i_{qr} \\ Q_s = \frac{3V_s}{2L_s} (V_s - M \omega_s i_{dr}) \end{cases} \quad (13)$$

A. RSC Control

In this work, the issues which need to be addressed by the RSC control are:

- Capture of maximum energy from the wind (MPPT);
- Power quality improvement, through power factor enhancement and harmonics current filtering.

From (10), the electromagnetic torque can be controlled directly by acting on i_{qr} current component. Then, the q-reference rotor current is given by:

$$I_{qr-active}^* = -\frac{2L_s}{3PMV_s} T_{em}^* \quad (14)$$

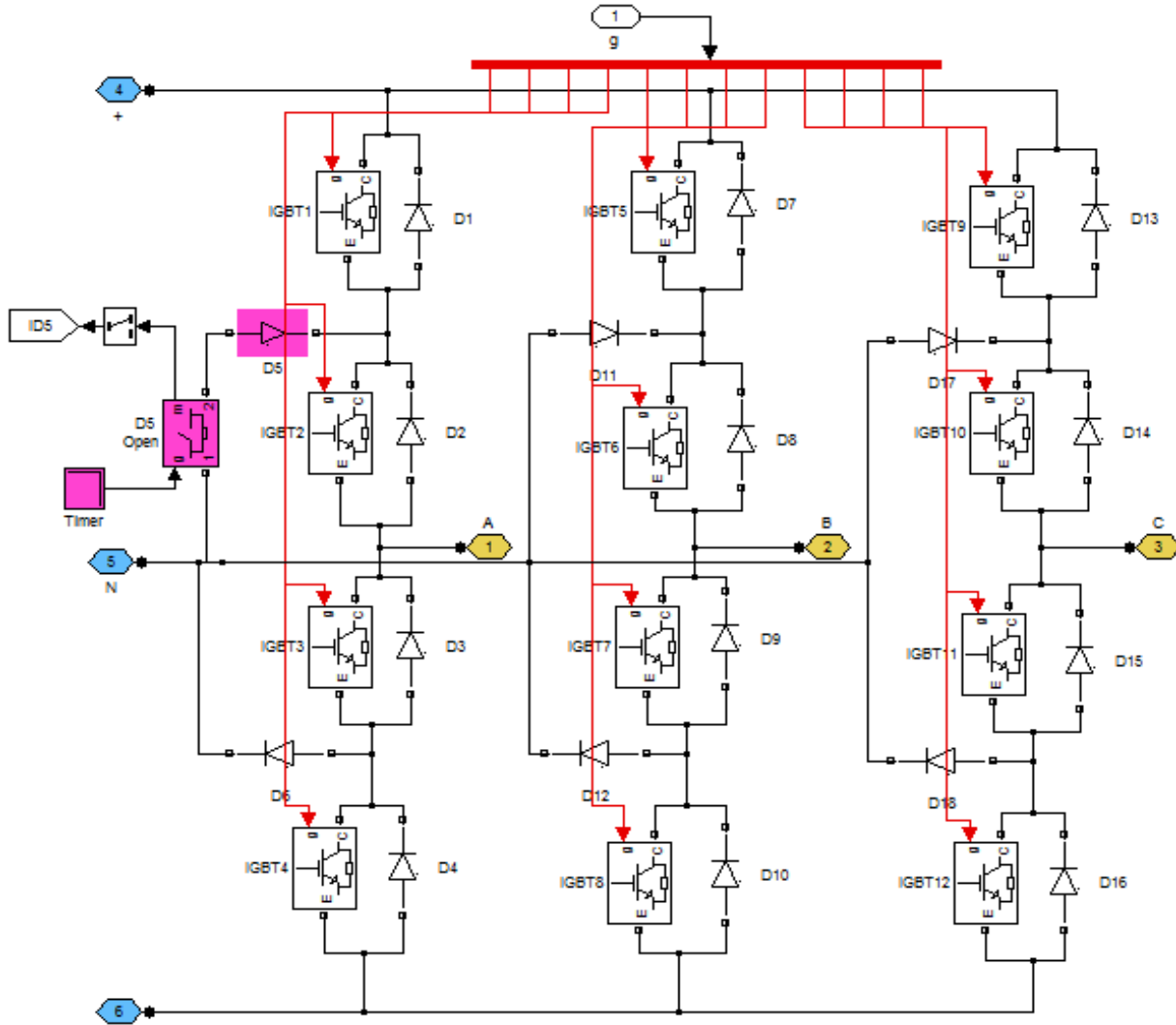


Fig. 4 Control scheme of the GSC for remove the rotor harmony

From (13), one can note that the stator reactive power can be controlled by acting on i_{dr} . Then, the d-reference rotor current is given by:

$$I_{dr-reactive}^* = -\frac{L_s}{MV_s} \left(\frac{2}{3} Q_s^* - \frac{V_s^2}{\omega_s L_s} \right) \quad (15)$$

To ensure the MPPT, a FLC has been used (see Fig. 5). In addition, to extract a maximum of power from the wind, the generator speed command is estimated by:

$$\Omega_g = \delta \frac{\lambda_{opt} V}{R} \quad (16)$$

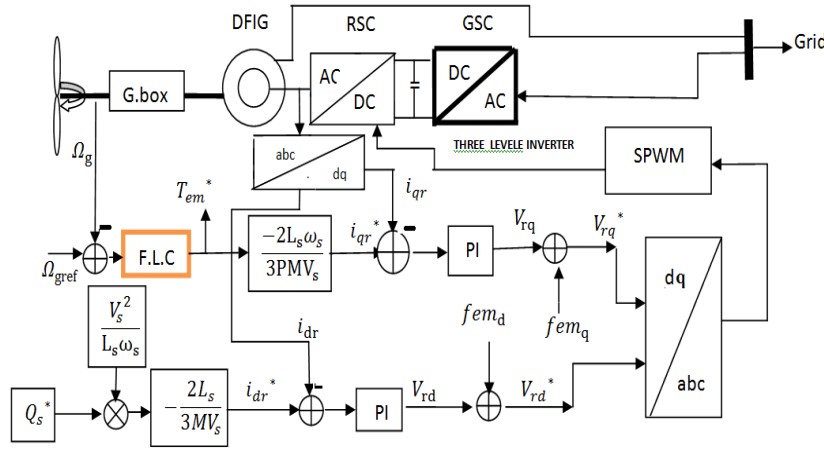


Fig. 5 Control scheme of the RSC for power generation and GSC for remove the rotor harmonic

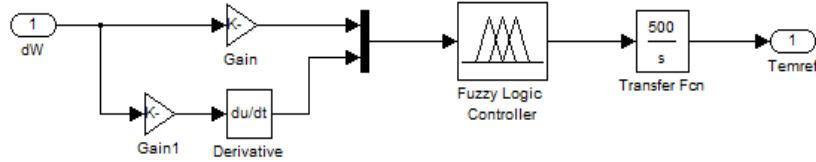


Fig. 6 Speed fuzzy controller

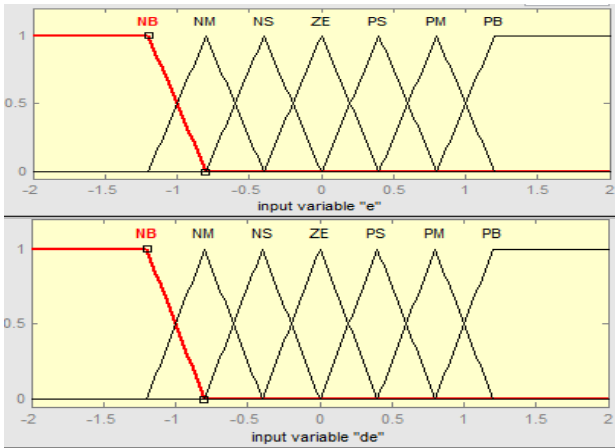


Fig. 7 Graphical representation of the fuzzy sets

B. Grid Side Converter Control

There exists harmonics rotor torsion between the stator

with δ is the gear box ratio and λ_{opt} is the optimum tip speed ratio. To control the RSC, the reference i_{qref} (see Fig. 5) is derived from the speed error e and its variation Δ_e by tuning the FLC. Also, to control the reactive power to a desired value, a command current i_{dref} is derived from (15), as shown in Fig. 4. Elsewhere, to design the current control loops along the two axes, (12) was used. The cross coupling terms between the d-axis and q-axis can be removed through a feed forward compensation. Thereby, by adding a PI regulator in the loop, the independent control of the d-axis and q-axis rotor currents is realized, as shown in Fig. 5.

terminals. The harmony of the non-integer multiples of the original frequency is less than the fundamental frequency. There is harmony between engine torsional loads. Due to changes in wind speed and the frequency variation in the rotor, result of passive filters is virtually impossible. Active filters are used to change the main component's frequency. The use of multilevel inverters is an effective way to remove the rotor harmonic. So, to remove frequency components below 40 Hz in side of stator, the three-level inverter and the fifth and eleventh harmonic feed rotor are used.

IV. SIMULATIONS RESULT

In this section, the wind speed is taken as constant value. Then, the maximum power extraction is not taken into account; the wind turbine is driven around synchronous generator speed (314 rad/s). The control strategy is applied to a WECS equipped with a 7.5 kW DFIG. The system parameters are given in the appendix. The switching

frequency of the RSC and the GSC is chosen equal to 10 kHz. The performance of the WECS ancillary services is studied under the nominal stator active power ($P_{sn} = 7.5 \text{ kW}$) for a nominal wind speed of 13.3 m/s. The total load of the system is composed of a non-linear wind speed experiences gusts.

A. Fuzzy Controller

The fuzzy controller used is shown on Fig. 6. It is the Mamdani controller based on 195 Max-Min method, modulated on MATLAB/Simulink software.

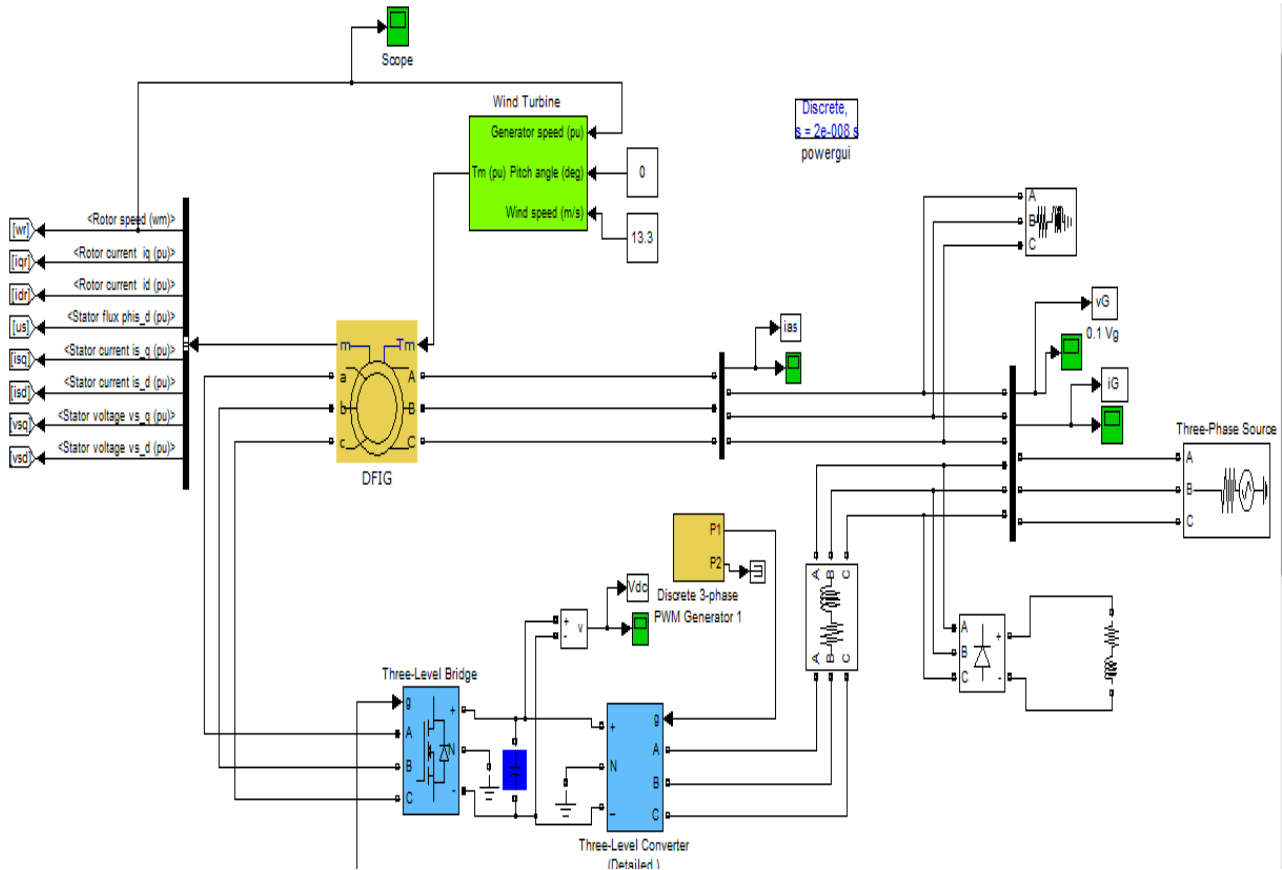


Fig. 8 Simulation scheme of a 7.5 kW DFIG wind turbine-generator system

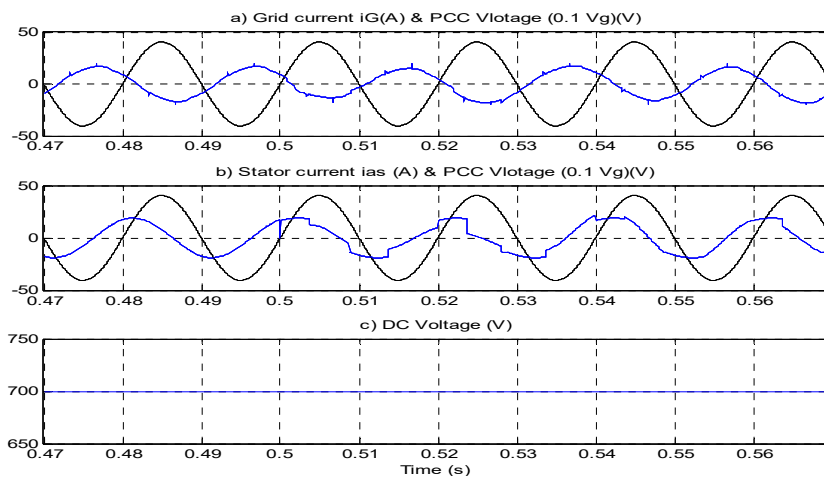


Fig. 9 Waveforms Grid current before and after compensation voltage point of common coupling (PCC) and dc voltage

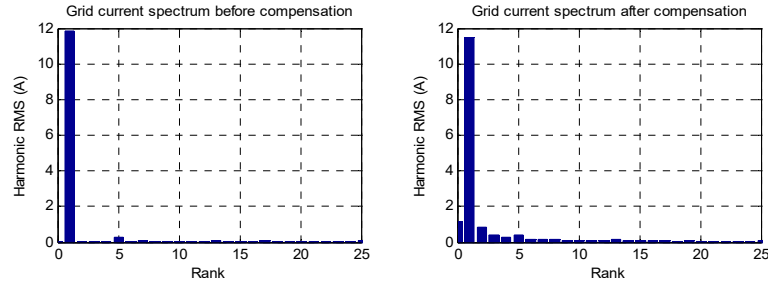


Fig. 10 Waveforms Grid current harmonic spectrum after and before compensation

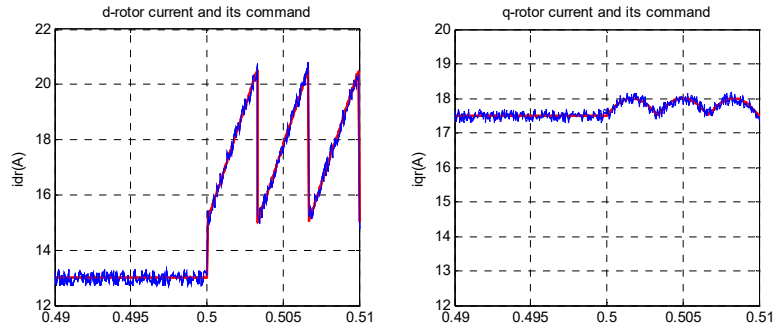
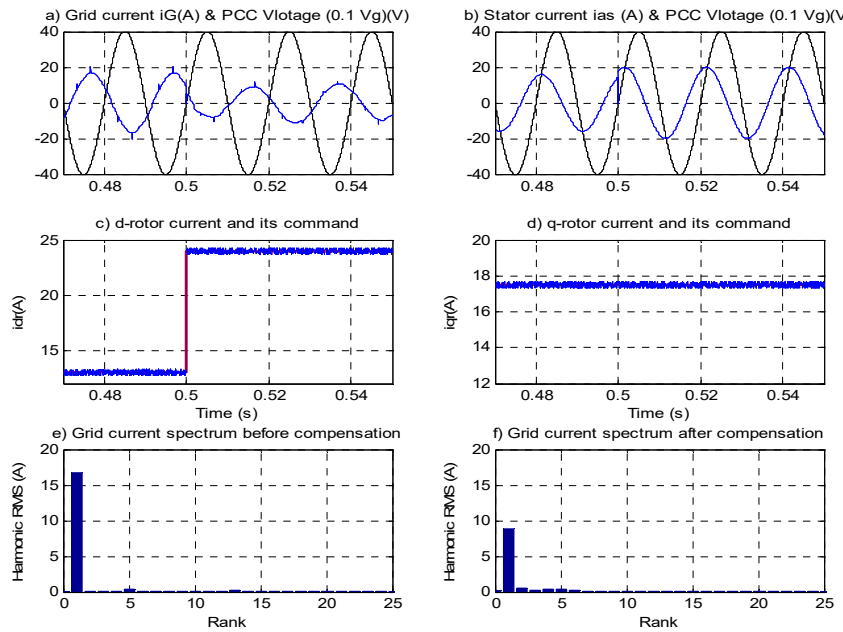


Fig. 11 Waveforms d-q current axis and reference signal

Fig. 12 Waveforms Grid current, d-q axis rotor current and PCC voltage ($0.1V_g$) after and before compensation

V. CONCLUSION

In this paper a technique has been presented for direct active and reactive power control of variable speed DFIG and power quality improvement of grid in presence of nonlinear load. To ensure the MPPT, a FLC has been used in RSC side. Three inverters in GSC side recompense PCC voltage through power factor enhancement and harmonics current filtering. Also, GSC control provides its unity power factor operation

and smooth DC link voltage. Simulation results prove effectiveness of method.

REFERENCES

- [1] Brahim Nait-kaci, Mamadou L. Doumbia, "Active and Reactive power control of a doubly fed induction generator for wind applications", IEEE 2009.
- [2] Arantxa Tapia, Gerardo Tapia, J. Xabier Ostolaza, "Modeling and Control of a Wind Turbine Driven doubly fed Induction Generator",

- IEEE 2003.
- [3] J. Ben Alaya, A. Khedher and M. F. Mimouni, "DTC, DPC and Nonlinear Vector Control Strategies Applied to the DFIG operated at Variable Speed", *Journal of Electrical Engineering (IEEE)*, vol.6, no II, pp. 744-753, 2011.
 - [4] A. Nassani, A. Ghazal, and A. L. Elshafei, "Speed sensorless control of DFIG based MRAS observer", 14th International Middle East Conference, pp. 476-481. 2010.
 - [5] A. Luna, F. K. A. Lima, P. Rodriguez, E. H. Watanabe and R. Teodorescu, "Comparison of Power Control Strategies for DFIG Wind Turbines", *IEEE Trans on Energy Conversion*, pp. 2131-2136, 2008.
 - [6] M. Singh, V. Khadkikar, A. Chandra. Grid synchronization with harmonics and reactive power compensation capability of a permanent magnet synchronous generator-based variable speed wind energy conversion system. *IET Power Electronics* 2011; 41:122e30.
 - [7] Z. Chen, Compensation schemes for a SCR converter in variable speed wind power systems. *IEEE Transactions on Power Delivery* 2004; 19:2813e21.
 - [8] S. Engelhardt, I. Erlich, C. Feltes, J. Kretschmann, F. Shewarega. Reactive power capability of wind turbines based on doubly fed induction generators. *IEEE Transactions on Energy Conversion* 2011; 26:1364e72.
 - [9] Kayikçi. M. J. Milanovic. Reactive power control strategies for DFIG-based plants. *IEEE Transactions on Energy Conversion* 2007; 22:389e96.
 - [10] M. Machmoum, A. Hatoum, T. Bouaouiche. Flicker mitigation of a doubly-fed induction generator for wind energy conversion system. *Mathematics and Computers in Simulation* 2010; 81:2433e45.
 - [11] M. Shahbazi, P. Poore, S. Saadate, M.R. Zalgadri. Five-leg converter topology for wind energy conversion system with doubly fed induction generator. *Renewable Energy* 2011; 36:113187e94.
 - [12] O. Soares, H. Gonçalves, A. Martins, A. Carvalho. Nonlinear control of the doubly fed induction generator in wind power systems. *Renewable Energy* 2010; 35:81662e70.
 - [13] F. Poitiers, T. Bouaouiche, M. Machmoum. Advanced control of a doubly-fed induction generator for wind energy conversion. *Electric Power Systems Research* 2009; 79:71085e96.
 - [14] T.K.A. Brekken, N. Mohan. Control of a doubly fed induction wind generator under unbalanced grid voltage conditions. *IEEE Transaction on Energy Conversion* 22 (March (1)) (2007) 129–135.
 - [15] Z. S., Changliang Xia, T. Shi. Assessing transient response of DFIG based wind turbines during voltage dips regarding main flux saturation and rotor deep-bar effect. *Applied Energy* 87 (2010) 3283–3293.
 - [16] A. Gaillard, P. Poure, S. Saadate, M. Machmoum. Variable Speed DFIG Wind Energy System for Power Generation and Harmonic Current Mitigation. *Renewable Energy* 34, 2009 pp 1545-1553.
 - [17] B. Robyns, B. Francois, P. Degobert, J. P. Hautier, Vector control of induction machines, Springer-Verlag London 2012.
 - [18] P.C. Krause Analysis of electric machinery. New York: McGraw-Hill; 1986.
 - [19] H. M. Jabr and N. C. Kar, "Neuro-fuzzy vector control for doubly-fed wind driven induction generator," in *Proc. of the IEEE Electrical Power Conference*, pp. 236 - 241, 2007.
 - [20] H. M. Jabr and N. C. Kar, "Leakage flux saturation effects on the transient performance of wound-rotor induction motor," *Journal of Electric Power Systems Research*, Vol.78, No.7, pp.1280-1289, 2008.